FOREWORD

This study was initiated by the Biophysics Laboratory of the 6570th Aerospace Medical Research Laboratories, Aerospace Medical Division, Wright-Patterson Air Force Base, Ohio. The research was conducted by the Northrop Space Laboratories, Hawthorne, California, under Contract No. AF 33(657)-11010. Mr. Robert E. Fortney, Member of the Research Staff, was the principal investigator for the Northrop Space Laboratories. Mr. Jerry D. Speakman, of the Environmental Stress Branch, Multienvironment Division, was the contract monitor for the Aerospace Medical Research Laboratories. The work was performed in support of Project No. 6301, "Aerospace Systems Personnel Protection," and Task No. 630101, "Physical Protection of Man Against Ionizing Radiation." The research sponsored by this contract was started in July 1963 and was completed in September 1963.

The authors gratefully acknowledge the assistance of Mr. M. R. Morrison and Mr. J. L. Spadafora.

Northrop Space Laboratories have assigned number NSL 63-172 to this document.

ABSTRACT

Radiation tolerance levels vary for the different vital body organs and, therefore, the radiation dose distribution in an astronaut may be critical in future space endeavors. This study was initiated to determine analytically the dose distribution inside a model astronaut. The basis of the mathematical formulation for determining this distribution is presented in this report. Particles of the ambient environment were assumed to impinge isotropically on the APOLLO Command Module (CM). The radiation was attenuated through a typical vehicle wall thickness and mean dose rates at various depths in a model astronaut were calculated. Four depths were investigated, each having approximately 175 points at which the dose was calculated. Two spectra were considered; one for Van Allen protons and the other representing solar flare protons. The results are presented in graphical form, giving dose versus depth in the model astronaut.

PUBLICATION REVIEW

This technical documentary report is approved.

J. W. HEIM
Technical Director
Biophysics Laboratory

TABLE OF CONTENTS

LIST OF FIGURES

INTRODUCTION

The Model Astronaut Dose Distribution Analysis (MADDA) is a mathematical analysis of space radiation dose as a function of depth in a model astronaut. Ambient space radiation spectra are assumed to impinge on the APOLLO Command Module (CM). The incident particles are attenuated and the spectra are modified in passing through the various slant thicknesses of wall material. The filtered proton spectra impinge on a model astronaut within the vehicle. The astronaut has been represented mathematically by two right elliptical cylinders; one cylinder representing the human torso and the other the neck and head. The particles are further attenuated as they penetrate the body tissue to the point in question. Radiation dose must be determined at several points in the model in order to obtain a mean value for a given depth. Repeating this procedure for different depths is necessary to determine the dose distribution in the model astronaut.

The development of the mathematical techniques and computer programs utilized in this study are formulated in reference 1.

ENVIRONMENT

Two components of the radiative environment are utilized in this analysis. They are the protons from the inner Van Allen zone and solar cosmic ray event protons. The spectrum for the Van Allen zone protons was developed by combining the curves of Freden and White, ref 2, and Naugle and Kniffen, ref 3. The composite spectrum has been normalized to 1 proton $cm^{-2}sec^{-1}ster^{-1}$ having $E > 40$ Mev, and is used in differential form, figure 1, in subsequent calculations.

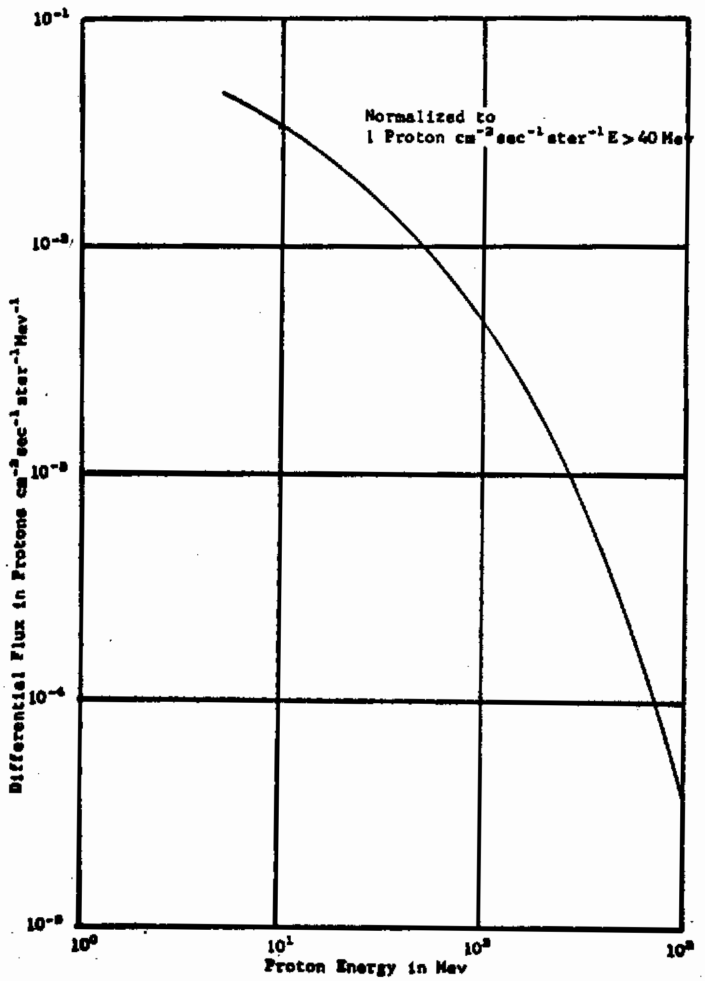

FIGURE 1 - Ambient Proton Spectrum
Within The Van Allen Zone

Because of the variability of individual solar flares, a "typical" spectrum cannot be utilized; instead an envelope flare has been constructed by plotting intensity versus time for most of the flares of this solar cycle ref 4. A curve of higher intensity than the peak of any single event represents the spectrum of an envelope flare. This spectrum has been normalized to 1 proton $cm^{-2} ster^{-1}$ having E > 100 Mev for use in the dose calculations. This solar flare spectrum is presented in figure 2.

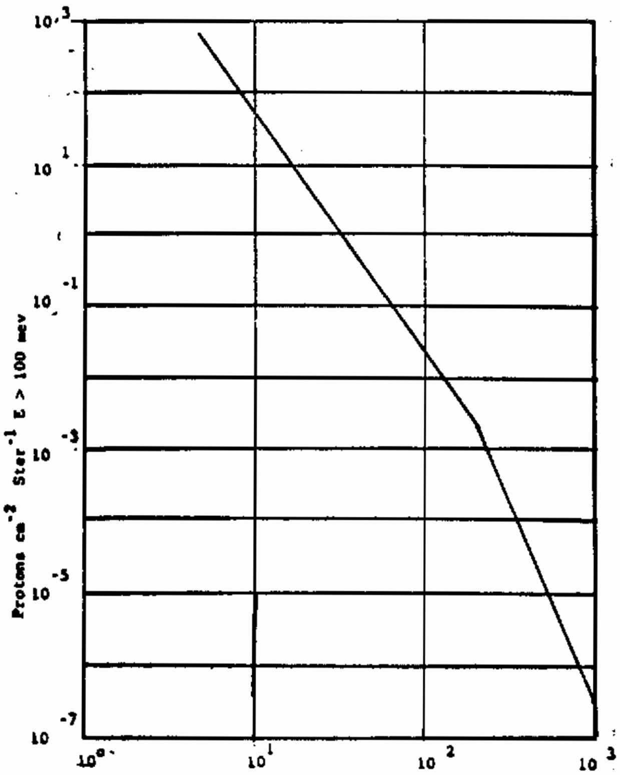

Figure 2 - Envelope Flare

APOLLO (CM) SPACE VEHICLE GEOMETRY

In this study an attempt was made to account for the stratified walls of the APOLLO (CM). The walls of the vehicle were assumed to be laminated, as illustrated in figure 3. Material densities and probable design thicknesses are also given on the figure. The thickness of the heat-resistant material, phenolic nylon, is variable since greater thicknesses are required on the blunt end and the lower side of the vehicle during re-entry. The thickness of phenolic nylon is assumed to vary as $[\sin(\frac{\psi}{2})]^4$. The angle ψ is equivalent to the angle θ in a cylindrical coordinate system with ψ measured in the YZ plane. The APOLLO design dimensions were obtained from NASA MSC, Houston, Texas.

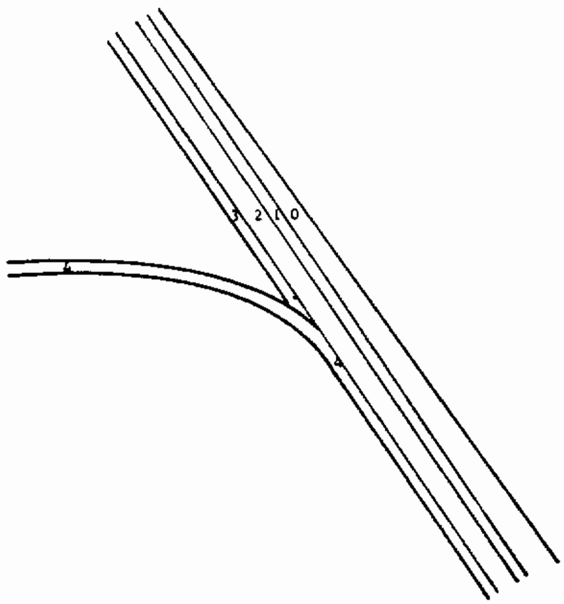

Layer Number	Material	ρ g/cm^3	Normal Inches	Thickness g/cm^2	Equivalent Thickness Weighting Factor
0	Phenolic Nylon	1.20150	Variable		1.221
1	Stainless Steel Backup	7.83344	.1	1.990	0.8403
2	Thermoflex Insulation	0.03845	.5	.004883	1.0582
3	Stainless Steel Shell	7.83344	.1	1.990	0.8403
4	Aluminum Pressure Vessel	2.768	.1	.7031	1.000

Figure 3 - Typical Wall Of The APOLLO Command Module (CM)

The technique used in describing the surface of the space vehicle is straightforward. The spacecraft is assumed to be represented by the combination of several geometrical surfaces. Analytical expressions for different surfaces are utilized. Spherical, conical, and toroidal surfaces are sufficient to describe the APOLLO (CM). The expressions for these surfaces are

Spherical

$$(x-a)^2 + (y-b)^2 + (z-c)^2 - R^2 = 0 \qquad (1)$$

Conical

$$\frac{z^2}{c^2} + \frac{y^2}{b^2} - \frac{(x-a)^2}{a^2} = 0 \qquad (2)$$

Toroidal

$$\left[(x-a)^2 + y^2 + z^2 + b^2 - r^2\right]^2 - 4b^2 \left(y^2 - z^2\right) = 0 \qquad (3)$$

where the various constants are as shown in figure 4.

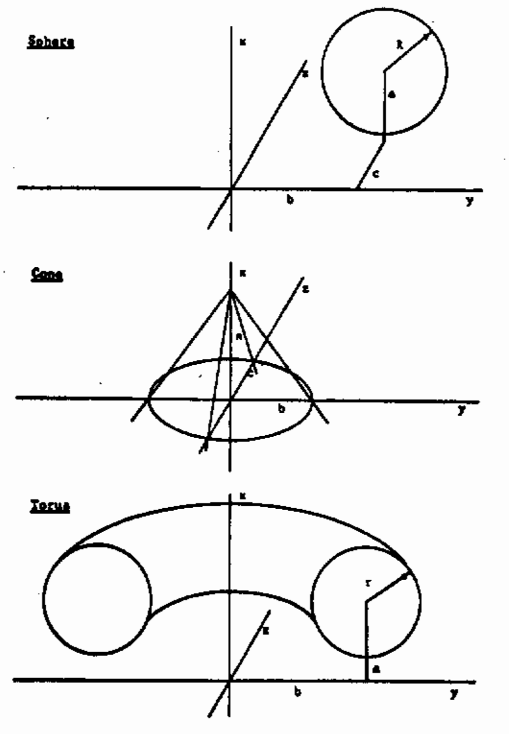

Figure 4 - Surfaces Available For Describing Spacecraft Geometry

In order to calculate the radiation dose at a point, the space about this point must be divided into incremental solid angles for integration purposes. Spherical coordinate angles θ and φ, defining rays representing each solid angle, are utilized in the calculation. The intersection points of these rays with the specified vehicle surfaces are then determined. The coordinates of the intersection points are given by

$$x = t \sin \varphi \cos \theta \quad (4)$$

$$y = t \sin \varphi \cos \theta \quad (5)$$

$$z = t \cos \varphi \quad (6)$$

The parameter t, in the above, is found by parametric substitution into the equations for the various surfaces. The resulting equations are in quadratic form and the solution for t is given by

$$t = \frac{-B_1 \pm \sqrt{B_1{}^2 - 4A_1 C_1}}{2A_1} \quad (7)$$

where

<u>Spherical</u>

$$A_1 = 1.0 \quad (8)$$

$$B_1 = -2 \; (a \sin \varphi \cos \theta + b \sin \varphi \sin \theta + c \cos \varphi) \quad (9)$$

$$C_1 = a^2 + b^2 + c^2 - R^2 \quad (10)$$

<u>Conical</u>

$$A_1 = a^2 b^2 \cos^2\varphi + a^2 c^2 \sin^2 \varphi \sin^2 \theta - b^2 c^2 \sin^2 \varphi \cos^2 \theta \quad (11)$$

$$B_1 = 2 \; ab^2 \; c^2 \; \sin \varphi \cos \theta \quad (12)$$

$$C_1 = -a^2 \; b^2 \; c^2 \quad (13)$$

<u>Toroidal</u>

$$A_1 = 1.0 \quad (14)$$

$$B_1 = -2 \; [a \sin \varphi \cos \theta + b \; (\sin^2\varphi \sin^2\theta + \cos^2\varphi)^{\frac{1}{2}}] \quad (15)$$

$$C_1 = a^2 + b^2 - r^2 \quad (16$$

The dose rate at a point within a satellite or astronaut will depend upon the amount of material the radiation must penetrate to reach the point. Material slant thicknesses representing each solid angle must be known in order to account for the radiation attenuation. The material slant thicknesses are calculated from the normal wall thicknesses.

The relationship between the vehicle wall slant thickness (T_s) and the normal thickness (T_n) can be seen in figure 5.

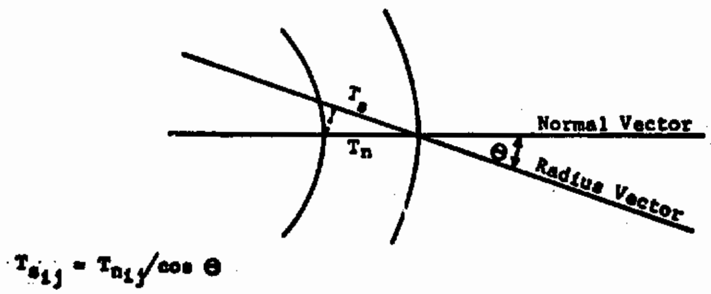

Figure 5 - Wall Slant Thickness Relationship

The formulation used in determining cos Θ is as follows:

$$\cos \Theta = \frac{\vec{N}}{|\vec{N}|} \cdot \frac{\vec{R}}{|\vec{R}|} = \cos \alpha_N \cos \alpha_R + \cos \beta_N \cos \beta_R + \cos \gamma_N \cos \gamma_R \quad (17)$$

where α, β, and γ are the direction angles of the vector normal to the vehicle surface ($\vec{N}$) and the radius vector ($\vec{R}$).

$$\cos \alpha_R = (x\text{-XREF})/\text{DEN} \quad (18)$$

$$\cos \beta_R = (y\text{-YREF})/\text{DEN} \quad (19)$$

$$\cos \gamma_R = (z\text{-ZREF})/\text{DEN} \quad (20)$$

$$\text{DEN} = \sqrt{(x\text{-XREF})^2 + (y\text{-YREF})^2 + (z\text{-ZREF})^2} \quad (21)$$

where x, y z = coordinates of intersection point

XREF, YREF, ZREF = coordinates of point at which the dose is to be calculated

Spherical

$$\cos \alpha_N = (x-a)/DEN \tag{22}$$

$$\cos \beta_N = (y-b)/DEN \tag{23}$$

$$\cos \gamma_N = (z-c)/DEN \tag{24}$$

$$DEN = \sqrt{(x-a)^2 + (y-b)^2 + (z-c)^2} \tag{25}$$

Conical

$$\cos \alpha_N = (a-x)/(a^2\ DEN) \tag{26}$$

$$\cos \beta_N = y/(b^2\ DEN) \tag{27}$$

$$\cos \gamma_N = z/(c^2\ DEN) \tag{28}$$

$$DEN = \sqrt{\left(\frac{a-x}{a^2}\right)^2 + \left(\frac{y}{b^2}\right)^2 + \left(\frac{z}{c^2}\right)^2} \tag{29}$$

Toroidal

$$\cos \alpha_N = [f(x,y,z)(x-a)]/DEN \tag{30}$$

$$\cos \beta_N = [f(x,y,z)y-2b^2 y]/DEN \tag{31}$$

$$\cos \gamma_N = [f(x,y,z)z-2b^2 z]/DEN \tag{32}$$

$$DEN = \sqrt{[f(x,y,z)(x-a)]^2+[f(x,y,z)y-2b^2y]^2+[f(x,y,z)z-2b^2z]^2} \tag{33}$$

$$f(x,y,z) = (x-a)^2 + z^2 + b^2 - r^2 \tag{34}$$

where the constants are as defined previously.

The angle Θ is seen to be a function of the position of the point in the astronaut. It must therefore be calculated for each point considered, while the intersection points on the surface of the vehicle are calculated only once.

MODEL ASTRONAUT

A vital part in the determination of dose distribution in an astronaut is the calculation of self shielding. A mathematical model representing an astronaut was devised and used to calculate tissue slant thicknesses. These thicknesses are then used along with the vehicle wall slant thicknesses to determine the dose rate per steradian penetrating various solid angles to reach a given point.

A mathematical model of an astronaut must reflect a certain amount of the details of the human body. To reflect the flatness of the human torso and head, yet maintain relatively simple geometry, two right elliptical cylinders were utilized to represent the astronaut. (See figure 6.) The larger cylinder represents the human torso while the smaller cylinder represents the neck and head. The dimensions of the model are input data in the program.

The dimensions of the model astronaut used in this study are based on mean dimensions of U. S. Air Force flying personnel. The torso, head and neck mean dimensions were obtained from ref 5, table 29-1.

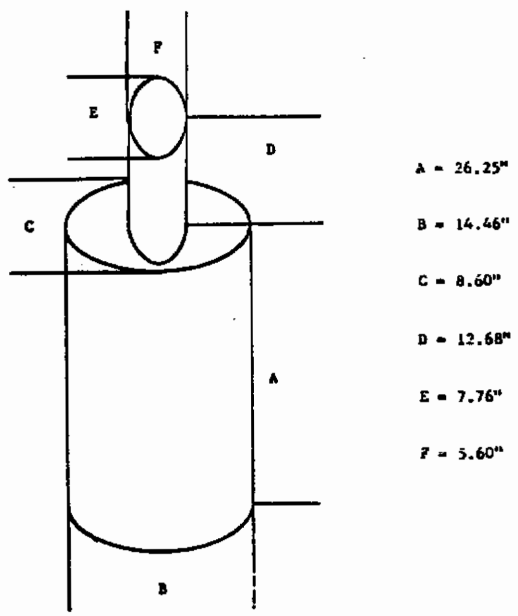

Figure 6 - Model Astronaut Based On Dimensions Of U. S. Air Force Flying Personnel

Torso

Height = Cervical height - crotch height =
59.08 - 32.83 = 26.25" (35)

$$\text{Minor Axis} = \frac{\text{Chest Depth + waist depth + buttock depth}}{3} =$$

$$\frac{9.06 + 7.94 + 8.81}{3} = 8.60'' \quad (36)$$

$$\text{Major Axis} = \frac{\text{Biacromial diameter + hip breadth}}{2} =$$

$$\frac{15.75 + 13.17}{2} = 14.46'' \quad (37)$$

Head and Neck

Height = sitting height - shoulder (acromial) height
(sitting) = 35.94 - 23.26 = 12.68" (38)

Minor Axis = Bitragion diameter = 5.60" (39)

Major Axis = Head length = 7.76" (40)

The self-shielding effects of the arms and legs are not included in this study.

Using the mathematical model astronaut described above, the intersection points of various rays on the elliptic and plane surfaces are calculated. This is similar to the calculations made for the vehicle.

Since the intersection points on the vehicle surface remain constant, the set of angles (θ_{ij} and φ_{ij}) defining the rays are different for each point. A set of angles, θ's and φ's, are computed according to

$$\varphi_{ij} = \cos^{-1}\left[\frac{z_{ij} - ZREF}{RV_{ij}}\right] \quad (41)$$

$$\theta_{ij} = \cos^{-1}\left[\frac{x_{ij} - XREF}{RV_{ij}\sin(\varphi_{ij})}\right] \quad (42)$$

where x_{ij}, z_{ij} = coordinates of intersection points on vehicle surface

XREF, ZREF = coordinates of reference point

RV_{ij} = radius vector from the reference point to a point on the surface

The equations for calculating the coordinates of the intersection points on the model astronaut surfaces are the same as before. The expressions for the parameter t are:

Plane

$$t = \frac{1}{A_1} \tag{43}$$

$$A_1 = \frac{\sin\varphi\cos\theta}{a} + \frac{\sin\varphi\sin\theta}{b} + \frac{\cos\varphi}{c} \tag{44}$$

Elliptical Cylinder

$$t = \frac{-B_1 \pm \sqrt{B_1^2 - 4A_1C_1}}{2A_1} \tag{45}$$

$$A_1 = b^2\cos^2\varphi + c^2\sin^2\varphi\sin^2\theta \tag{46}$$

$$B_1 = -2\,C\,b^2\cos\varphi - 2\,c^2\,B\sin\varphi\sin\theta \tag{47}$$

$$C_1 = b^2C^2 + c^2B^2 - b^2c^2 \tag{48}$$

The angles θ and φ are those which are calculated by equations 41 and 42.

A major part of the computation time is concerned with determining which intersection points are valid and which are not. Since the mathematical descriptions of the surfaces are for infinite lines, planes, and elliptical cylinders, many of the intersections are not true points. A test is made first to see if an intersection is on the right end of a ray. If an intersection point is on one of the planes it must be on or within the elliptical boundaries. Intersection points on the elliptical surfaces must lie between the proper planes. Still other tests are made to determine if a ray passes through both the torso and the head and if so, where it enters and leaves the head.

Once a point is found to be valid it is a simple matter to calculate tissue thicknesses (TIS_{ij}).

$$TIS_{ij} = \sqrt{x^2 + y^2 + z^2} \tag{49}$$

If a ray passes through both torso and head the values are merely added to get the total tissue thickness.

PROTON PENETRATION

The differential proton spectra, figures 1 and 2, are utilized as input data for the Proton Shielding Program, ref 6. The incident spectra are attenuated by various thicknesses of aluminum (in slab geometry) and the emerging spectra of protons and neutrons are determined by the program. Some of the spectra are shown in figure 7 along with the original Van Allen proton spectrum for comparison. The computer program described in ref 6, assumes that the energy of the proton may be expressed as

$$E(E_o, X) = E_o + S(E)X \qquad E_o > 200 \text{ Mev} \tag{50}$$

or

$$E(E_o, X) = E_o \left(1 - \frac{X}{R(E_o)}\right)^n \qquad E_o \leq 200 \text{ Mev} \tag{51}$$

where

$E(E_o, X)$ = the proton energy at depth X of protons having initial energy E_o, Mev,

E_o = the initial proton energy, Mev,

$S(E)$ = the stopping power for proton of energy E,

or $-\frac{1}{\rho}\frac{dE}{dx}$ in gm/cm^2,

X = depth of penetration, gm/cm^2,

$R(E_o)$ = range of proton energy E_o,

and n = exponent which is a function of material,

The above is based on ionization loss, while the inelastic collisions are handled as

$$E_s = \frac{E'' - E^*}{\text{Yield}} \text{ or } \frac{E''' - E^*}{\text{Yield}} \tag{52}$$

where

E_s = energy of emitted secondary neutron or proton,

E^* = excitation energy resulting from nuclear interaction,

E'' and E''' = energy of proton or neutron interacting with the nucleus,

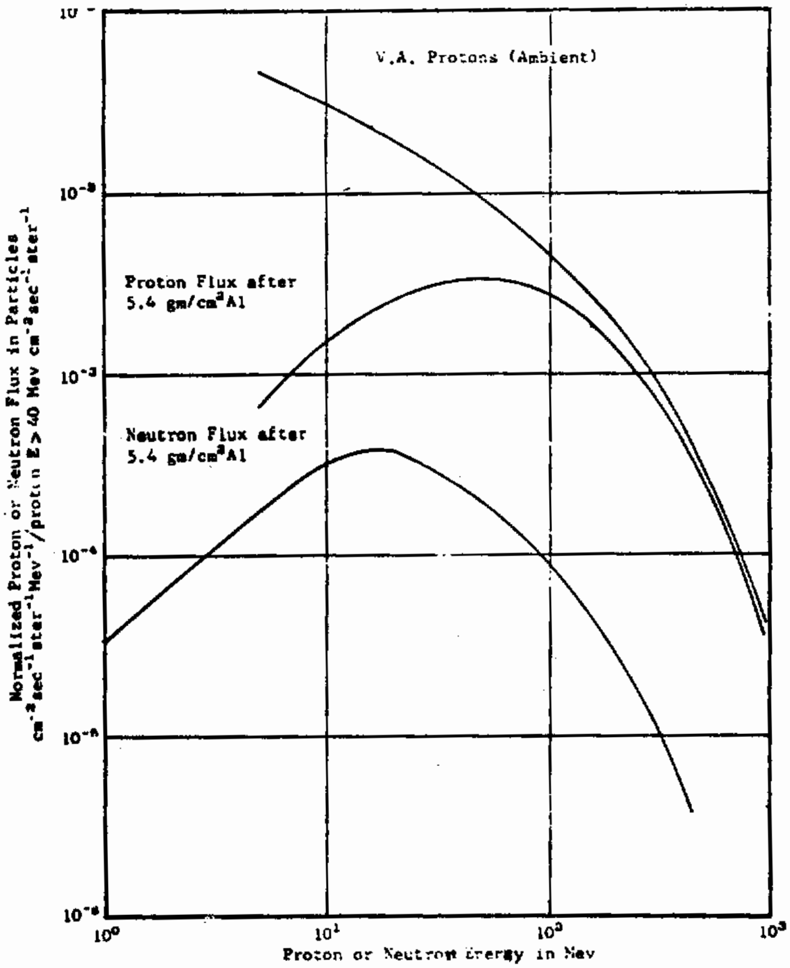

Figure 7 - Differential Spectra Of Protons And Neutron Produced When Van Allen Protons Penetrate 5.4 gm/cm² Of Aluminum

$$\text{Yield} = \begin{cases} Y_{pp} + Y_{np}/R_{pn} & \text{(for secondary protons)} \\ Y_{pn} R_{pn} + Y_{nn} & \text{(for secondary neutrons),} \end{cases}$$

R_{pn} = energy of emitted proton/energy of emitted neutrons,

and

Y_{ij} = ratio of j particles produced per i particle interaction.

The proton flux is then formulated as

$$\varphi_p(E, X + \Delta X) = \varphi_p(E', X) \frac{\Delta E'}{\Delta E} e^{-\Delta X/\lambda}$$

$$+ Y_{pp} [\varphi_p(E'', X) \frac{\Delta E''}{\Delta E} F_p(E'')]$$

$$+ Y_{np} [\varphi_n(E''', X) \frac{\Delta E'''}{\Delta E} F_n(E''')] \quad (53)$$

where

$\varphi_p(E, X+\Delta X)$ = Differential proton flux of protons at energy E exiting from $(X+\Delta X)$ due to inelastic collisions from $\varphi_n(E''', X)$ in ΔX,

$\varphi_p(E'', X)$ = Differential proton flux of protons at energy E'' at depth X where E'' gives rise to secondary protons of energy E,

$\varphi_n(E''', X)$ = Differential flux of neutrons at energy E''' at depth X where E''' gives rise to secondary protons of energy E,

$F_p(E'')$ = Fraction of protons which undergo inelastic reactions such that secondary protons escape from ΔX,

$F_n(E''')$ = Fraction of neutrons which undergo inelastic reactions such that secondary protons escape from ΔX,

and $\Delta E'$, $\Delta E''$, and $\Delta E'''$ are energy decrements which are utilized as ratios to ΔE to maintain conservation of flux. These expressions give the results illustrated on figure 7.

DOSE CALCULATIONS

Proton dose rate calculations in this analysis are based on the Van Allen proton spectrum, figure 1, and the envelope solar flare proton spectrum, figure 2. The first spectrum is assumed to be constant throughout the inner Van Allen zone and, therefore, a normalized spectrum was used in the penetration calculations. The integrated flux encountered on a particular space flight could be determined by the Trajectory and Environment Program (ref 7) and would provide a dose multiplication constant. The envelope solar flare spectrum represents time integrated differential flux and is also normalized. Although a dose multiplication constant is needed for the flare, it is not discussed here.

The Proton Shielding Program is used to determine the proton spectrum penetrating a slab of shielding material. The program assumes that the impinging flux is normal to the surface of the slab, similar to the illustration in figure 8a. Parts b and c of figure 8 depict a sphere and spherical shell of the same shielding material in isotropic flux fields. Assuming straight-ahead penetration, the computed dose rate at point P_1 is equivalent to dose rates at points P_2 and P_3 due to the basic definition of flux. The dose rate at Point P_4, however, is quite different, since much of the radiation arriving at this point must penetrate larger thicknesses of the shielding material.

Calculations of radiation dose rates for each wall and tissue thickness combination using shielding programs would require considerable computer time. The approach used here has been to use the shielding programs independently to generate curves of dose rate versus tissue thickness for various vehicle wall thicknesses. These curves are then fit with an orthogonal polynomial expression of the form

$$\ln \quad \text{Dose Rate} = [A_1 + A_2 t^1 + A_3 t^2 + \ldots A_n t^{n-1}] \qquad (54)$$

where

t = tissue thickness, g/cm^2

A_n = set of coefficients which is a function of the wall thickness

The coefficients in the above expression have been determined for several thicknesses of aluminum. Six terms were used in this study and the results for Van Allen protons are given in table I. Figure 9 illustrates the curves which are represented by the ten sets of coefficients in table I.

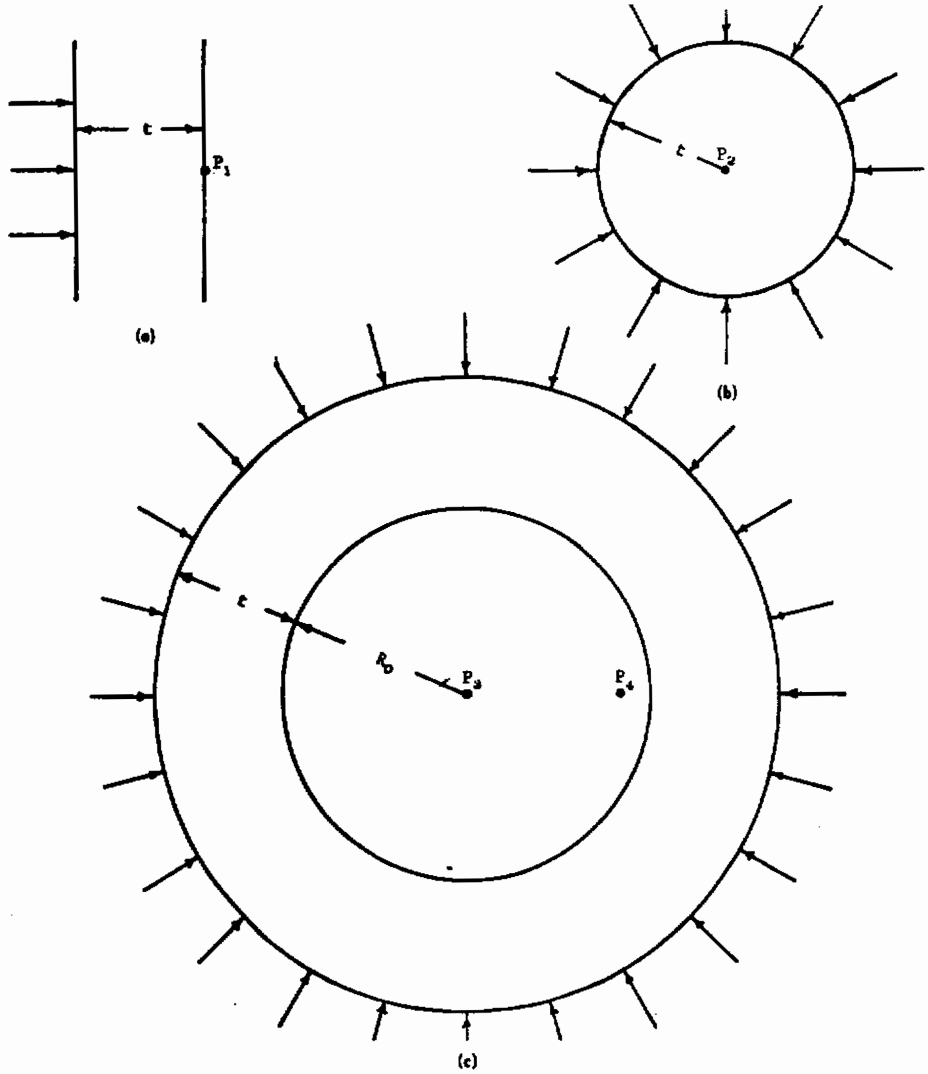

Figure 8 - Flux Geometry Relationships

In general, the calculated wall slant thicknesses will fall between two of the fitted curves. A good approximation of dose rate for each wall-tissue thickness combination is found by interpolation between the adjacent curves. In the event that the calculated wall thickness is outside the range of the input values, the curve corresponding to the nearest thickness is used.

The total dose rate at a given point is found by summation over all space utilizing the expression

$$D_n = \sum_{ij} D_{ij} \, \Delta \Omega_{ij} \tag{55}$$

where

D_{ij} = dose rate per steradian about point n

$\Delta\Omega_{ij}$ = incremental solid angle about point n

TABLE I

ORTHOGONAL POLYNOMIAL COEFFICIENTS FOR VARIOUS THICKNESSES OF ALUMINUM

N	Al Thickness g/cm^2	A(N,1)	A(N,2)	A(N,3)	A(N,4)	A(N,5)	A(N,6)
1	3.0	-0.77537×10^{1}	-1.26944×10^{-1}	$+3.28078 \times 10^{-3}$	-4.92462×10^{-5}	$+3.54788 \times 10^{-7}$	-9.71000×10^{-1}
2	5.0	-0.79985×10^{1}	-1.07907×10^{-1}	$+2.63945 \times 10^{-3}$	-3.93649×10^{-5}	$+2.84616 \times 10^{-7}$	-7.83595×10^{-1}
3	7.5	-0.82309×10^{1}	-0.94998×10^{-1}	$+2.22540 \times 10^{-3}$	-3.29698×10^{-5}	$+2.39033 \times 10^{-7}$	-6.62063×10^{-1}
4	10.0	-0.84561×10^{1}	-0.82255×10^{-1}	$+1.90224 \times 10^{-3}$	-2.87687×10^{-5}	$+2.11131 \times 10^{-7}$	-5.87674×10^{-1}
5	12.5	-0.85453×10^{1}	-0.77621×10^{-1}	$+1.73046 \times 10^{-3}$	-2.57371×10^{-5}	$+1.86741 \times 10^{-7}$	-5.15556×10^{-1}
6	15.0	-0.86865×10^{1}	-0.69078×10^{-1}	$+1.43559 \times 10^{-3}$	-2.07702×10^{-5}	$+1.48205 \times 10^{-7}$	-4.04536×10^{-1}
7	17.5	-0.88534×10^{1}	-0.61138×10^{-1}	$+1.19336 \times 10^{-3}$	-1.70385×10^{-5}	$+1.21369 \times 10^{-7}$	-3.32586×10^{-1}
8	20.0	-0.90702×10^{1}	-0.48813×10^{-1}	$+0.78841 \times 10^{-3}$	-1.05579×10^{-5}	$+0.73264 \times 10^{-7}$	-1.98954×10^{-1}
9	25.0	-0.93125×10^{1}	-0.35567×10^{-1}	$+0.37735 \times 10^{-3}$	-0.39198×10^{-5}	$+0.22070 \times 10^{-7}$	-0.50493×10^{-1}
10	30.0	-0.95070×10^{1}	-0.28949×10^{-1}	$+0.24334 \times 10^{-3}$	-0.26444×10^{-5}	$+0.16651 \times 10^{-7}$	-0.42634×10^{-1}

The procedure is then repeated for several points on a surface at a given depth. After calculating the dose rate at a specified number of points the mean dose is determined for this depth in the model astronaut. The points are assumed to represent areas on a surface and the mean dose rate is found by

$$\bar{D}_t = \frac{\sum_n D_n A_n}{\sum_n A_n} \tag{56}$$

where

$\bar{D}_t$ = mean dose rate at depth t in the model astronaut

D_n = calculated dose rate for nth point on surface at depth t

A_n = area of surface at depth t represented by nth point

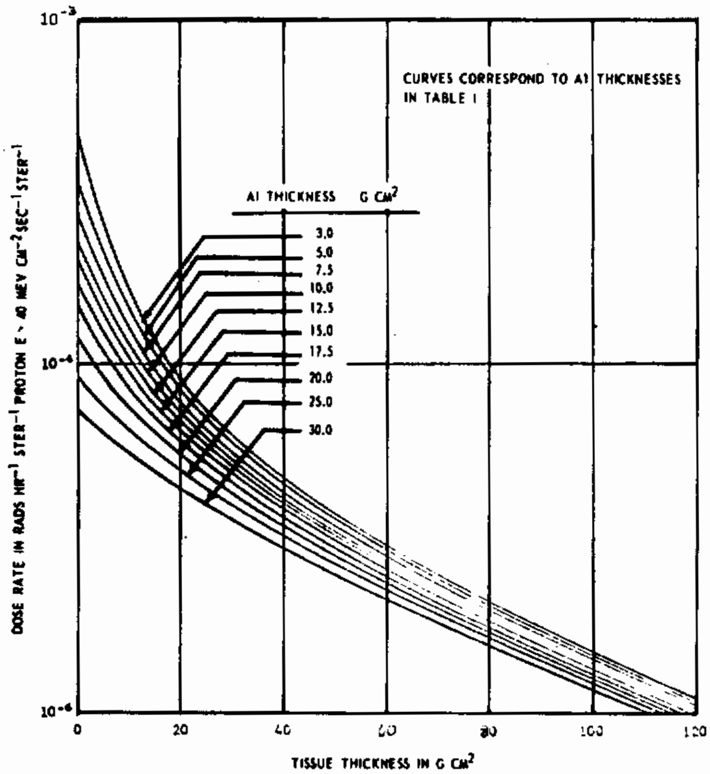

Figure 9 - Dose Rate Versus Depth In Tissue Due To Van Allen Protons After Passing Through Various Thicknesses Of Aluminum

RESULTS

Dose distributions in the model astronaut due to Van Allen protons and solar flare protons have been determined for the model located at the center of the APOLLO (CM). Mean doses were calculated for four different depths in the model, utilizing approximately 175 points at each depth and 342 solid angles about each point. The resulting dose distributions are presented in figures 10 and 11.

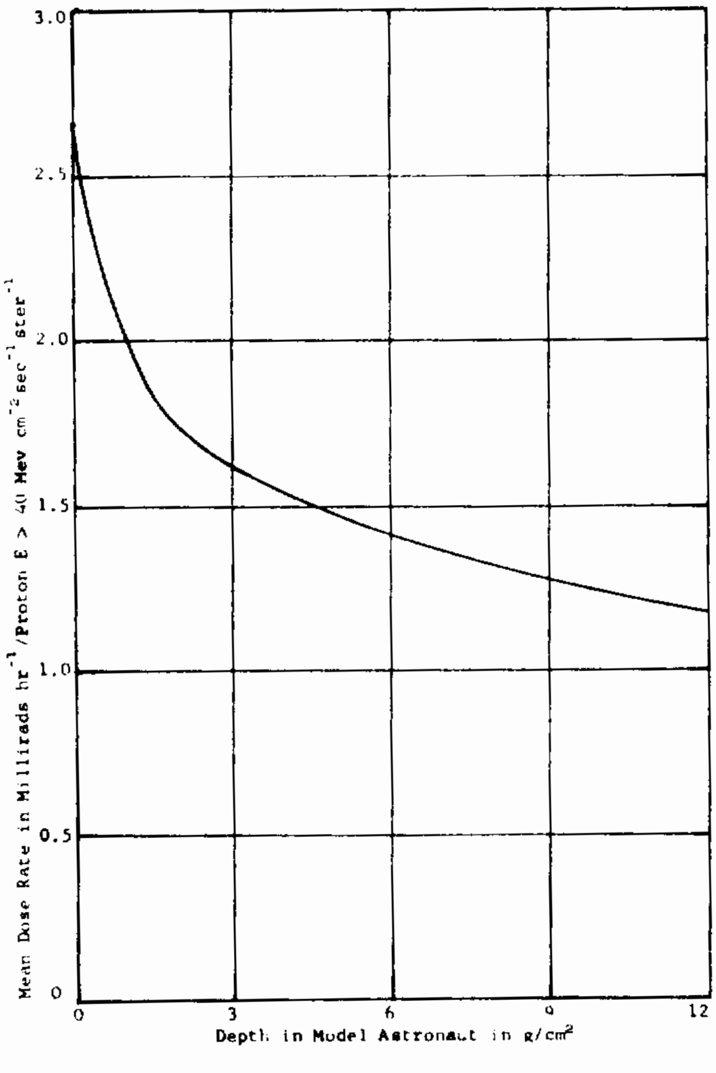

Figure 10 - Model Astronaut Dose Distribution Due to Van Allen Protons Filtered By The APOLLO (CM)

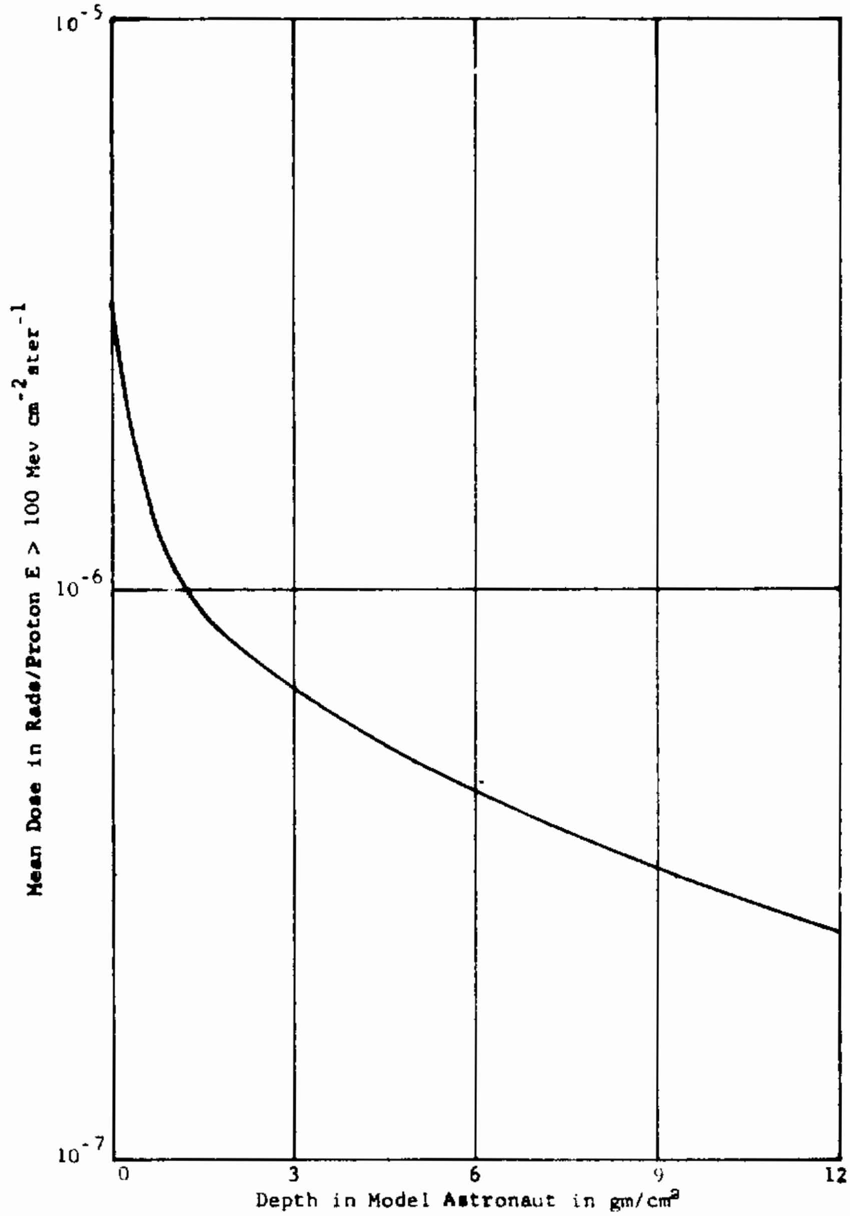

Figure 11 - Model Astronaut Dose Distrubution Due To Solar Flare Protons Filtered By The APOLLO (CM)

REFERENCES

1. Fortney, R. E., Computer Analysis of Radiation Shielding, Report No. AMRL-TDR-64-11, 6570th Aerospace Medical Research Laboratories, Wright-Patterson AFB, Ohio, February 1964.

2. Freden, S. C. and White, R. S., Trapped Proton and Cosmic-Ray Albedo Neutron Fluxes, University of California Report, UCRL-6603, October 2, 1961.

3. Naugle, J. E. and Kniffen, D. A., "Variations of the Proton Energy Spectrum with Position in the Inner Van Allen Belt," Journal of Geophysical Research, Vol. 68, 13, pp. 4065-4078, July 1, 1963.

4. Solar Proton Manual, ed., McDonald, F. B., X-611-62-122, NASA, Goddard Space Flight Center, Greenbelt, Md., January 1963.

5. Hansen, R., Cornog, D. Y., Hertzberg, H. T. E., "Annotated Bibliography of Applied Physical Anthropology in Human Engineering," WADC TR 56-30, Wright Air Development Division, Wright-Patterson Air Force Base, Ohio, May 1958.

6. Fortney, R. E., and Duckworth, G. E., Proton Shielding Program for the IBM 7090, NSL 62-81, Northrop Space Laboratories, Hawthorne, California, May 1962.

7. Morrison, M. R., and Tate, A. E., Determination of Particle Fluxes Impinging on a Spacecraft, NSL 63-63R-1, Northrop Space Laboratories, Hawthorne, California, AF 33(657)-8762, August 1963.